Characterization of Solvent and Deuterium Isotope Effects on Nonadiabatic Proton Transfer in the Benzophenone/*N*,*N*-Dimethylaniline Contact Radical Ion Pair

Kevin S. Peters* and Ganghyeok Kim

Department of Chemistry and Biochemistry, University of Colorado, Boulder, Colorado 80309-0215

Received: November 11, 2003; In Final Form: January 21, 2004

The dynamics of proton transfer within a variety of substituted benzophenones/*N*,*N*-dimethylaniline contact radical ion pairs are examined in a wide range of solvent polarities. The correlation of the rate constants with the thermodynamic driving force reveals both a normal and inverted region for proton transfer in solvents with an E_T30 value of less than 43.1; in solvents with E_T30 greater than 43.8, only the normal region is observed. Also, the kinetic deuterium isotope effect is examined. The solvent and isotope dependence for the transfer process is examined within the context of the Lee−Hynes model for nonadiabatic proton transfer. The theoretical analysis of the experimental data suggests that the reaction path for proton transfer involves tunneling. Conventional transition state theory with the inclusion of tunneling in the region of the transition state cannot account for the observed kinetic behavior.

Introduction

Although in recent years there have been significant advances in our understanding of the importance of solvent in controlling reaction dynamics, the effects of solvent upon proton-transfer processes are less well understood.[1−7] The standard theory employed in the analysis of the dynamics for proton/deuteron transfer has been the semiclassical model, which is based upon transition-state theory with the inclusion of tunneling in the region of the transition state.[8,9] Recently the basic tenet of transition-state theory, as applied to proton-transfer reactions, has been brought into question.[1,4,10−24] Theoretical studies suggest that when there is an electronic barrier in the proton-transfer coordinate, instead of the proton passing over the barrier through thermal activation, the proton tunnels through the barrier, giving rise to a nonadiabatic transfer process.[1] In the current theories for nonadiabatic proton transfer, as in nonadiabatic electron transfer, it is the reorganization of the solvent about the reacting system that brings the reactant and product states into resonance, which is integral to the transfer process. Thus, to test these theories for nonadiabatic proton transfer, it is important that molecular systems be employed that allow for the examination of the reaction processes in a wide range of solvents.

The photochemical reduction of benzophenone by *N*,*N*-dimethylaniline is a molecular system that is well suited for the study of intermolecular nonadiabatic proton transfer.[22] By employing a variety of substituted benzophenones, the thermodynamic driving force for the reaction can be varied over a range of 10 kcal/mol. Furthermore, the proton-transfer process occurs in solvents of wide ranging polarity. Also, the distance of proton transfer in the triplet radical ion pair is constrained due to the π-stacked nature of the triplet complex.[22] Thus, benzophenone/*N*,*N*-dimethylaniline is a useful molecular system for assessing the validity of nonadiabatic proton-transfer theory.

Recently we reported a kinetic study for proton transfer in the benzophenone/*N*,*N*-dimethylaniline triplet radical ion pair system in series of four nitrile solvents.[24] The dynamics of proton transfer were examined within the context of Lee−Hynes theory for nonadiabatic proton transfer.[15] For the nitrile solvents, Lee−Hynes theory gave a good account of the observed kinetic behavior. In the present paper, we extend our analysis of applicability Lee−Hynes theory by examining the dynamics of proton transfer in a variety of solvents that span a wider range in solvent polarity. In addition, we examine the theoretical predictions of the Lee−Hynes model for the kinetic deuterium isotope effect.

Experimental Section

The solvents tetrahydrofuran, ethyl acetate, 1,2-dichloroethane, and dimethyl sulfoxide were obtained from Aldrich and used as received. Benzophenone, 4-chlorobenzophenone, 4-fluorobenzophenone, 4-methylbenzophenone, 4-methoxybenzophenone, and 4,4′-dimethoxybenzophenone were obtained from Aldrich, and 4,4′-dimethylbenzophenone was obtained from Kodak. Each was recrystallized from ethanol. *N*,*N*-Dimethylaniline (Aldrich) was distilled from calcium hydride under reduced pressure and stored under argon.

N,*N*-Dimethyl-d_6-aniline was prepared by the condensation of freshly distilled aniline with CD_3OD and P_2O_5.[25] Aniline (25.8 g) was added over 30 min to a mixture of CD_3OD (50 g) and P_2O_5(133.7 g), and the mixture was heated to 150 °C for 15 h. After cooling, 94 mL of 10 M NaOH was added and then followed by the addition of Na_2CO_3, producing a pH of 9.0. The aqueous solution was diluted by an equal volume of H_2O, which was then followed by four diethyl ether extractions of equal volume. After drying over $MgSO_4$, filtration, and removal of the ether solvent, to the residue was added 1.5 mL of acetic anhydride, which was then distilled under aspirator vacuum. The NMR spectrum of the distilled product, 10 g, indicated $>99\%$ CD_3.

The picosecond laser system employs a Continuum (PY61C-10) producing a 19 ps pulse width. The apparatus for determining picosecond absorption kinetics as well as transient absorption spectra has been previously described.[26] A 1 cm flow cell was employed, which was maintained at 23 °C. The samples were irradiated at 355 nm, and the ensuing dynamics were monitored at 680 nm, which reflects the time dependence of the various subsituted benzophenone radical anions. Transient absorption spectra were monitored over the wavelength span of 420−760 nm.

10.1021/jp031237v CCC: $27.50
Published on Web 03/16/2004

TABLE 1: Rate Constants, k_{pt} ($\times 10^9$ s^{-1}), for Proton Transfer in Substituted Benzophenone−*N*,*N*-Dimethylaniline Triplet Contact Radical Ion Pairs

	DiOMe	DiMe	OMe	Me	H	F	Cl	Cl, Cl
tetrahydrofuran	2.6[a]	4.3	4.5	5.4	6.5	6.8	7.2	6.4
ethyl acetate	2.6	4.6	4.3	5.0	5.4	5.2	5.1	4.8
1,2-dichloroethane	2.1	3.1	2.9	3.6	4.1	3.7	3.4	2.9
pentanenitrile	2.7	3.8	3.6	4.2	4.2	4.1	3.1	
butanenitrile	3.2	4.3	4.0	4.3	3.9	3.9	2.9	
DMF	1.9	1.8	1.7	1.5	0.7	0.5	0.3	
propanenitrile	4.3	4.1	4.0	3.8	2.9	2.6	1.8	
DMSO	1.2	0.8	0.8	0.6	0.4			
acetonitrile	3.9	2.9	2.9	2.3	1.3	1.0	0.7	

[a] Estimated uncertainties in rate constants ±10% (1σ).

SCHEME 1

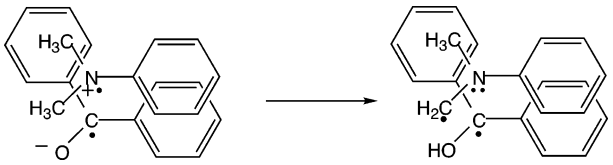

Some of the molecular parameters contained within Lee−Hynes theory are the vibrational frequencies of the proton/deuteron stretch and bend in the reactant and product states. Since these vibrational frequencies are experimentally unknown, the vibrational frequencies for *N*,*N*-dimethylaniline radical cation and the benzophenone ketyl radical were determined by the perturbative Becke−Perdew model (pBP/DN**) using MacSpartan Pro; the derived values for the vibrational frequencies were scaled by a factor of 0.9.[27]

Results and Discussion

Reaction Pathways. The photochemistry for the reaction mixture of 0.02 M benzophenone−0.4 M *N*,*N*-dimethylaniline (DMA) has been well characterized.[28] The 355 nm irradiation of benzophenone produces the first excited singlet state (S_1) which decays to the first excited triplet state (T_1), absorbing at 525 nm, on the 10 ps time scale. In the presence of 0.4 M *N*,*N*-dimethylaniline, the triplet state of benzophenone in acetonitrile is quenched by the transfer of an electron from *N*,*N*-dimethylaniline to form a contact triplet radical ion pair composed of the radical anion of benzophenone and the radical cation of DMA. The formation of the radical anion of benzophenone, monitored at 680 nm, occurs with a rate 8.3×10^9 s^{-1} for 0.4 M DMA. Employing higher concentrations of DMA leads to quenching of the first excited singlet state of benzophenone by electron transfer, producing a singlet contact radical ion pair; thus, higher concentrations of amine are to be avoided in order to simplify the kinetic analysis. Finally, the triplet contact radical ion pair decays by the transfer of a proton from the radical cation of DMA to the radical anion of benzophenone to form a contact triplet radical pair with unit efficiency on the 750 ps time scale; no other major decay channels are available to the contact triplet radical ion pair on the subnanosecond time scale in nonpolar solvents (Scheme 1).

In polar solvents, diffusional separation of the contact radical ion pair to form the solvent-separated radical ion pair is competitive with proton transfer.[28] Therefore, the kinetic modeling of the experimental data in polar solvents must account for both proton transfer, k_{pt}, and radical ion pair diffusional separation, k_{dif}.

$$\mathrm{RP} \xleftarrow{k_{pt}} \mathrm{CRIP} \xrightarrow{k_{dif}} \mathrm{SSRIP}$$

For the solvents tetrahydrofuran, ethyl acetate, and 1,2-dichloroethane, the rates of radical ion pair diffusional separation, k_{dif}, are all less than 1×10^8 s^{-1}. For dimethyl sulfoxide, $k_{dif} = 5 \times 10^8$ s^{-1}. The rates of proton transfer, k_{pt}, are given in Table 1. In addition, the rates of proton transfer in the series of nitrile solvents as well as dimethylformamide, obtained in a prior study, are included for comparison.[24] An example of the kinetic behavior for benzophenone, 4,4′-dimethylbenzophenone, and 4,4′-dimethoxybenzophenone in the presence of 0.4 M DMA in ethyl acetate is shown in Figure 1.

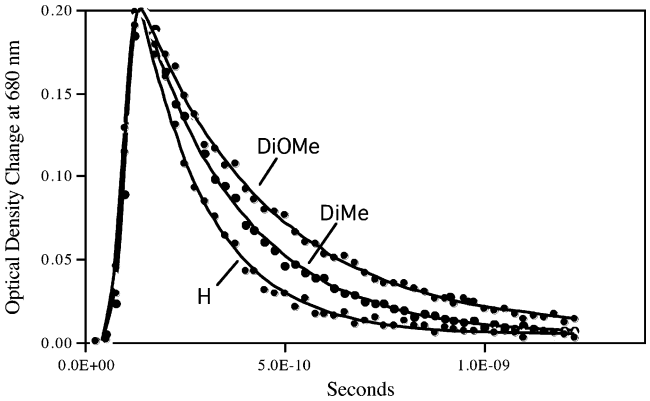

Figure 1. Transient absorption at 680 nm following the 355 nm excitation of 0.02 M dimethoxybenzophenone/0.4 M DMA (DiOMe), 0.02 M dimethylbenzophenone/0.4 M DMA (DiMe), and 0.02 M benzophenone/0.4 M DMA (H) in ethyl acetate: k_{pt}(DiOMe) = 2.6×10^9 s^{-1} and k_{dif}(DiOMe) = 1.0×10^8 s^{-1}, k_{pt}(DiMe) = 4.6×10^9 s^{-1} and k_{dif}(DiMe) = 1.0×10^8 s^{-1}, k_{pt}(H) = 5.4×10^9 s^{-1} and k_{dif}(H) = 1.0×10^8 s^{-1}, pulse width 19 ps, $t_0 = 97$ ps. Key: squares, experimental points; solid lines, fit to data.

TABLE 2: Rate Constants, k_{dt}, for Deuteron Transfer in Substituted Benzophenone/Dimethylaniline Triplet Contact Radical Ion Pairs and Kinetic Deuterium Isotope Effects, k_{pt}/k_{dt}

compound		pentanenitrile		butanenitrile	
4	**4′**	k_{dt} ($\times 10^9$ s^{-1})[b]	k_{pt}/k_{dt}	k_{dt} ($\times 10^9$ s^{-1})	k_{pt}/k_{dt}
CH_3O	CH_3O	2.4	1.1	2.7	1.2
CH_3	CH_3	2.7	1.4	2.9	1.5
CH_3O	H	2.8	1.3	3.0	1.3
CH_3	H	2.8	1.5	2.8	1.5
H	H	2.4	1.7	2.3	1.7
F	F	2.1	2.0	1.8	2.2
Cl	H	1.8	1.7	1.4	2.1

[a] Estimated uncertainties in rate constants ±10% (1σ).

The kinetic deuterium isotope effect on the transfer of a proton in the benzophenone/*N*,*N*-dimethyl-d_6-aniline contact triplet radical ion pair was examined in the solvents pentanenitrile and butanenitrile. The rate constants for proton transfer, k_{pt}, and deuteron transfer, k_{dt}, for the two solvents are given in Table 2. An example of the kinetic data for the deuterium isotope effect for 4-methylbenzophenone in pentanenitrile is shown in Figure 2.

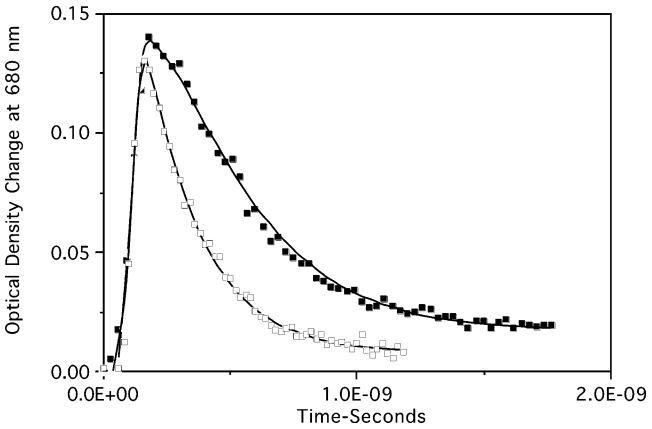

Figure 2. Transient absorption at 680 nm following the 355 nm excitation of 0.02 M 4-methylbenzophenone in the presence of 0.4 M *N*,*N*-dimethylaniline (open squares) and 0.4 M *N*,*N*-dimethyl-d_6-aniline (closed squares) in pentanenitrile. Fits (solid lines) for proton transfer, $k_{pt} = 3.8 \times 10^9\ s^{-1}$ and $k_{dif} = 2 \times 10^8\ s^{-1}$, and for deuteron transfer, $k_{dt} = 2.7 \times 10^9\ s^{-1}$ and $k_{dif} = 2 \times 10^8\ s^{-1}$, with pulse width 19 ps and $t_0 = 95$ ps.

Energy Analysis. The energetics for proton transfer within the contact radical ion pair to produce the triplet radical pair have not been directly measured and therefore can only be estimated through a thermodynamic analysis. The procedure for their determination has been outlined in an earlier publication.[22] It has recently been brought to our attention that more reliable values for the oxidation potential of DMA and the enthalpy for formation of the ketyl radical are available;[29,30] these new values serve to increase the overall driving force for proton transfer relative to those previously reported.[22−24] Therefore, the energetics of proton transfer and their variation with substituent and solvent are rederived.

The free energy of the benzophenone−DMA contact radical ion pair in acetonitrile relative to initial reactants, ΔG_{CRIP}, is obtained from the oxidation potential of DMA and the reduction potential of benzophenone through the relationship

$$\Delta G_{CRIP} = (E_D^{OX} - E_A^{RED}) + \Delta_{CRIP} \qquad (1)$$

where Δ_{CRIP} is the solvent correction based upon the Onsager dipole model.[31] The oxidation potential of DMA, E_D^{OX}, is 0.843 V vs SCE,[29] and the reduction potential of benzophenone, E_A^{RED}, is −1.86 V vs SCE.[32] The value of Δ_{CRIP} is obtained from the Gould, Goodman, Farid, and co-workers study of the solvent dependence of the energetics for contact radical ion pair of 1,2,4,5-tetracyanobenzene/hexamethylbenezene obtained through the analysis of the solvent dependence of their emission spectra.[31] We have taken their values for Δ_{CRIP} and developed a correlation with E_T 30. From the correlation, the derived value of Δ_{CRIP} for acetonitrile is +0.6 kcal/mol. Thus, the free energy for the formation of the contact radical ion pair of benzophenone/DMA from reactants is 62.9 kcal/mol. This value is somewhat higher than the value of 59.3 kcal/mol previously reported in the literature that we employed in our earlier studies.[31]

The free energy of the triplet radical pair is determined from the enthalpy for the addition of a hydrogen atom, −110.8 kcal/mol, to the triplet state of benzophenone, 69.2 kcal/mol, and the C−H bond dissociation enthalpy of DMA, 91.7 kcal/mol, yielding a triplet radical pair free energy of 50.1 kcal/mol (69.2 kcal/mol + 91.7 kcal/mol − 110.8 kcal/mol) above the ground-state reactants.[30] The change in entropy due to spin statistics on going from the initial reactants to the triplet radical pair is

SCHEME 2

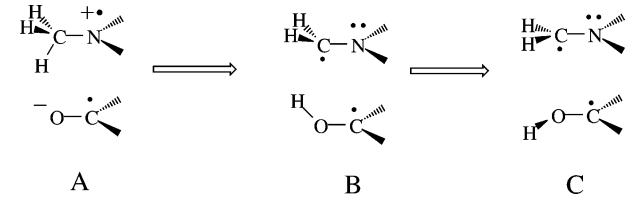

R ln 3, which at ambient temperatures is less than 1 kcal/mol and thus is neglected in the determination of the energetics.

In an earlier publication we speculated that structure for the reacting contact radical ion pair is that of a π-stack.[22] This structure leads to constraints in the proton motion and thus the ensuing product (Scheme 2).

The shortest distance for proton tunneling out of the reactant state A, Scheme 2, into the product state is for the product state to have the molecular structure B depicted in Scheme 2. After proton transfer, the B conformation relaxes by a 90° rotation to the equilibrium geometry of the product state, the C conformation (Scheme 2). The calculated value of 50.1 kcal/mol for the energy of the triplet radical pair corresponds to the radical pair having structure C. On the basis of pBP/DN** calculations, the B conformation is 3.4 kcal/mol higher in energy relative to C conformation of the benzophenone ketyl radical and represents a transition state for O−H rotational isomerization. Thus, the energy of the product state, B, that is relevant to proton transfer has an energy of 53.5 kcal/mol (50.1 kcal/mol + 3.4 kcal/mol) above the ground-state reactants.

The variation of the free energy of the contract triplet ion pair with substituent has been discussed previously.[22] The changes in free energy for the contact radical ion pair upon the addition substituents are 4,4′-dimethoxy (4.4 kcal/mol), 4,4′-dimethyl (2.1 kcal/mol), 4-methoxy (2.1 kcal/mol), 4-methyl (0.9 kcal/mol), 4-fluoro (−0.5 kcal/mol), 4-chloro (−1.9 kcal/mol), and 4,4′-dichloro (−4.0 kcal/mol). Combining these values with solvent dependence of Δ_{CRIP} obtained from the E_T30 correlation yields the energy of the contact radical ion pairs as a function of solvent (Table 3).

The substituent effect upon the energy of the triplet radical pair has been discussed.[22] Their values, assumed to be independent of solvent, are 4,4′-dimethoxy (0.4 kcal/mol), 4,4′-dimethyl (0.2 kcal/mol), 4-methoxy (0.2 kcal/mol), 4-methyl (0.1 kcal/mol), 4-fluoro (−0.1 kcal/mol), 4-chloro (0.1 kcal/mol), and 4,4′-dichloro (0.2 kcal/mol). Combining these values for the free energy of the triplet radical pair, structure B in Scheme 2, with free energy of the contact radical ion pairs shown in Table 3 allows for the driving force for proton transfer to be deduced (Table 4).

The procedure for investigating the mechanism of proton transfer involves the correlation of the rate constant for the transfer with the change in free energy. As the free energy change for proton transfer is varied through changes in substituents, it is assumed that the reacting species in each instance is the triplet contact radical ion pair. However, the derived energies for some of the contact radical ion pairs place them above the corresponding triplet state of the ketone (Table 3). For example in benzene, the calculated energy for the contact radical ion pair composed of 4,4′-dimethoxybenzophenone radical anion and DMA radical cation is 71 kcal/mol above the ground-state reactants while the triplet state of 4,4′-dimethoxybenzophenone is placed at 69.9 kcal/mol.[30] Thus, the triplet state is lower in energy than the calculated contact radical ion pair and may become involved in the reaction with DMA. However, the values for the energy of the contact radical ion pairs given

TABLE 3: Free Energy for Formation (kcal/mol) of Triplet Contact Radical Ion Pair for Substituted Benzophenone/DMA Relative to Ground-State Reactants and Triplet-State Energy for Ketone (kcal/mol)

	DiOMe	DiMe	OMe	Me	H	F	Cl	Cl, Cl
triplet-state energy[a]	69.9	69.2	69.0	69.2	69.2	*b*	*b*	*b*
cyclohexane	74	71.7	71.7	70.6	69.7	69.2	67.4	65.7
benzene	71	68.7	68.7	67.6	66.7	66.2	64.4	62.7
tetrahydrofuran	69.2	66.9	66.9	65.8	64.9	64.4	62.6	60.9
ethyl acetate	69.1	66.8	66.8	65.7	64.8	64.3	62.5	60.8
1,2-dichloroethane	68	65.7	65.7	64.6	63.7	63.2	61.4	59.7
pentanenitrile	67.8	65.5	65.5	64.4	63.5	63.0	61.2	59.5
butanenitrile	67.7	65.4	65.4	64.3	63.4	62.9	61.1	59.4
DMF	67.6	65.3	65.3	64.2	63.3	62.8	61.0	59.3
propanenitrile	67.5	65.2	65.2	64.1	63.2	62.7	60.9	59.2
DMSO	67.3	65.0	65.0	63.9	63.0	62.5	60.7	59.0
acetonitrile	67.2	64.9	64.9	63.8	62.9	62.4	60.6	58.9

[a] Taken from ref 30. [b] No reported value.

TABLE 4: Free Energy Change ($-\Delta G$, kcal/mol) for Proton Transfer within of Triplet Contact Radical Ion Pair for Substituted Benzophenone/DMA

	DiOMe	DiMe	OMe	Me	H	F	Cl	Cl,Cl
cyclohexane	20.1	18.0	18.0	17.0	16.2	15.8	13.9	10.0
benzene	17.1	14.6	14.6	14.0	13.2	12.8	10.9	9.4
tetrahydrofuran	15.3	13.2	13.2	12.2	11.4	11.0	9.1	7.6
ethyl acetate	15.2	12.8	12.8	12.1	11.3	10.9	9.0	7.5
1,2-dichloroethane	14.1	12.0	12.0	11.0	10.2	9.8	7.9	6.4
pentanenitrile	13.9	11.8	11.8	10.8	10.0	9.6	7.7	6.2
butanenitrile	13.8	11.7	11.7	10.7	9.9	9.5	7.6	6.1
DMF	13.7	11.6	11.6	10.6	9.8	9.4	7.5	6.0
propanenitrile	13.6	11.5	11.5	10.5	9.7	9.3	7.4	5.9
DMSO	13.4	11.3	11.3	10.3	9.5	9.1	7.2	5.7
acetonitrile	13.3	11.2	11.2	10.2	9.4	9.0	7.1	5.6

in Table 3 have errors of several kcal/mol and therefore cannot be used unequivocally to define the energy of the reacting species and thus its identity. Therefore, it is necessary for the reacting state to be directly determined. To this end we have examined the transient absorption spectra of many of the substituted benzophenone/DMA reacting species.

Transient Absorption Spectra. The transient absorption spectrum at 50 ps following the 355 nm irradiation of 0.02 M benzophenone/0.4 M DMA in acetonitrile is shown in Figure 3. This spectrum has previously been characterized and consists

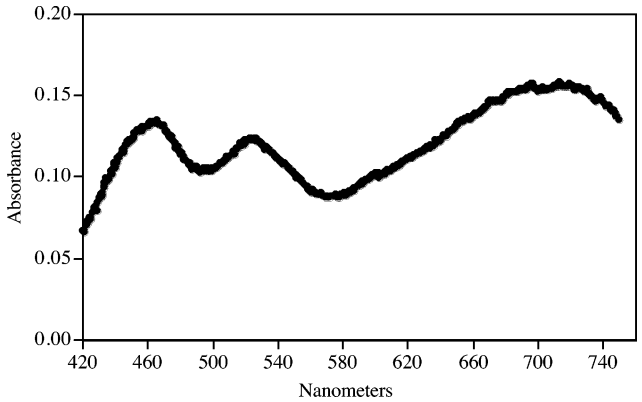

Figure 3. Transient absorption spectrum at 50 ps following the 355 nm irradiation of 0.02 M benzophenone/0.4 M DMA in acetonitrile.

of three species: the triplet state of benzophenone at 525 nm, the radical cation of DMA at 460 nm, and the radical anion of benzophenone at 710 nm.[28,33] The triplet state of benzophenone is still present at 50 ps as the rate constant for the quenching of the triplet state in the presence of 0.4 M DMA is 8.3×10^9 s^{-1}.[26]

The transient absorption spectra at 50 ps following the 355 nm irradiation of 0.02 M 4,4′-dimethoxybenzophenone/0.4 M DMA in the solvents pentanenitrile, benzene, and cyclohexane are shown in Figure 4. In pentanenitrile, three transient species

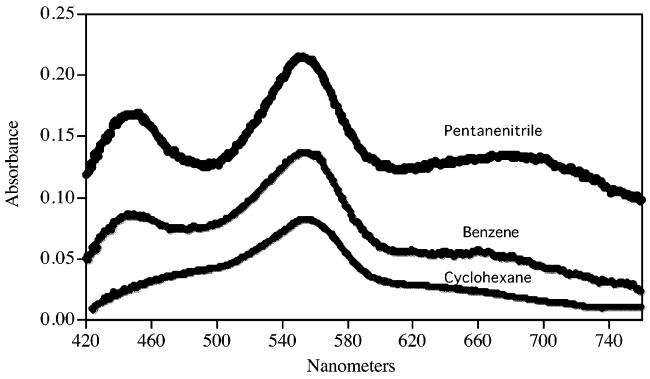

Figure 4. Transient absorption spectrum at 50 ps following the 355 nm irradiation of 0.02 M 4,4′-dimethoxybenzophenone in pentanenitrile, benzene, and cyclohexane.

are again observed—the triplet state of 4,4′-dimethoxybenzophenone at 550 nm, the radical cation of DMA at 450 nm, and the radical anion of 4,4-dimethoxybenzophenone at 690 nm. The shift in the spectrum of the radical cation of DMA to 450 nm from 460 nm observed in the benzophenone experiment is attributed to the shifting the triplet-state spectrum from 525 to 550 nm. In benzene, the same three transient species are observed, although the concentration of radical cation and radical anion have decreased at 50 ps due to a decrease in rate of electron transfer in the quenching of the triplet state of 4,4′-dimethoxybenzophenone as the solvent is changed from pentanenitrile to benzene. Finally, in cyclohexane at 50 ps, there is no evidence for the radical anion/radical cation pair as only the triplet state is observed. Similar behavior is found for 4,4′-dimethylbenzophenone and 4-methoxybenzophenone in these three solvents as well as the solvents tetrahydrofuran and ethyl acetate.

These experiments lead us to conclude that for the solvents employed in the present study the reacting species is the triplet radical cation/radical anion pair whose dynamics are monitored at 680 nm. In an earlier study employing benzene as the solvent, the reacting species again is the radical cation/radical anion pair. Although the above thermodynamic analysis places the 4,4′-dimethoxybenzophenone/DMA radical ion pair at 71 kcal/mol above the triplet state of 4,4′dimethoxybenzophenone at 69.9 kcal/mol, the reacting species is the radical ion pair, suggesting that the calculated value of 71 kcal/mol is too high. There is no evidence for an exciplex intervening in these reactions as the reacting species in benzene for the radical cation of DMA has the same absorption maximum in benzene and pentanenitrile. However, in cyclohexane, there is no evidence for radical ion pair for 4,4′-dimethoxybenzophenone, 4,4′-dimethylbenzophenone, and 4-methoxybenzophenone, and thus there is not a clear case for simple proton transfer in cyclohexane which instead may involve exciplex chemistry or direct hydrogen atom transfer. Therefore, our previous discussion of the inverted region for proton transfer in cyclohexane is not valid.[20]

Vibrational Analysis. If the B configuration is the state into which the proton tunnels, then it is the vibrations of B that will govern the rate of proton tunneling. Two vibrations are potentially active: the O−H stretch with associated frequency of 2386 cm^{-1} and the in-plane O−H bend with associated frequency of 768 cm^{-1}, both values determined by pBP/DN** calculations. The low value for the O−H stretch in the B conformation is attributed to the hyperconjugation of the radical with the O−H bond for in the B conformation the O−H bond is aligned parallel with the p-orbital containing the radical. The first overtone in the O−H stretch should not make a significant contribution to the tunneling rate in the B configuration as increasing the vibrational excitation by one quantum increases the effective O−H bond length, which serves to increase the distance for the proton to tunnel out of the A configuration and into the B configuration. A similar argument can be made for vibrational excitation of the O−H bending mode.

Lee−Hynes Model. In 1996, Lee and Hynes[15] presented a kinetic theory for nonadiabatic proton transfer that was based on the earlier developments of Borgis and Hynes.[1] The central tenet for nonadiabatic proton transfer is that when a proton encounters an electronic barrier in the transfer coordinate, the proton tunnels through the electronic barrier instead of thermally surmounting the electronic barrier. A condition for effective proton tunneling is that the reactant state and product state are in resonance at the time of the transfer. In the liquid phase, resonance of the two states is achieved by a fluctuation in the solvent structure about the reacting species, similar to processes found in nonadiabatic electron transfer. The contribution of solvent reorganization to the dynamics of proton transfer is reflected in the solvent reorganization energy parameter, E_s.

Another important parameter governing the rate of nonadiabatic proton transfer is the vibrational modulation of the distance between the two heavy atoms that bound the transferring proton. Borgis and Hynes originally suggested that the tunneling term for intermolecular proton transfer depends critically upon a low-frequency vibrational mode Q, with an associated frequency ω_Q that serves to reduce the two heavy atom internuclear separation.[11] As the distance of transfer decreases, the tunneling matrix element increases exponentially where the rate of increase is governed by a length parameter α. For nonadiabatic proton transfer the values of α's range from 25 to 35 $Å^{-1}$.[1] In nonadiabatic electron transfer, the electronic coupling matrix element has a corresponding length term of order of 1 $Å^{-1}$. Consequently, the proton tunneling matrix element is much more sensitive to the modulation of distance by intermolecular vibrations when compared to electron transfer. This phenomenon produces an additional energy term not found in electron transfer theory, E_α, defined as

$$E_\alpha = h^2\alpha^2/2m \tag{2}$$

where m is the reduced mass associated with vibration Q.

The rate constant for nonadiabatic transfer of the proton out of the n_r vibrational level in the reactant state into the m_p vibrational level in the product state, as formulated by Lee and Hynes, is given by[15]

$$k(n_r \rightarrow m_p) = k_{m_p,n_r}(0)(\pi/2A_2)^{1/2}\exp(-A_1^{\,2}/2A_2) \tag{3}$$

where $k_{m_p,n_r}(0)$, A_1, and A_2 are defined as

$$k_{m_p,n_r}(0) = 2(2\pi/h)^2[C_{m_p,n_r}(Q)]^2\exp\{(E_\alpha/h\omega_Q)2\coth(\beta h w_Q/2)\}$$

$$A_1 = (2\pi/h)\{\Delta E + E_s + E_Q + E_\alpha + [hm_P\omega_P - hn_R\omega_R] + 2\Delta Q/|\Delta Q|\,(E_\alpha E_Q)^{1/2}\coth(\beta h\omega_Q/2)\}$$

$$A_2 = 2(2\pi/h)^2k_BT\{E_s + (E_\alpha + E_Q)(\beta h\omega_Q/2\pi\coth)\{\beta h\omega_Q/2\pi\} + \Delta Q/|\Delta Q|(E_\alpha E_Q)^{1/2}(\beta h\omega_Q)\}$$

In the above expression, ω_R and w_P are the vibrational frequencies associated with the nth level of reacting proton in the reactant state and the mth level in the product state, and ω_Q is the frequency associated with the low-frequency mode developed in the Borgis−Hynes model. The term ΔQ reflects the change in equilibrium distance between the reactant and product states, and the energy associated with the reorganization is E_Q. The driving force for the reaction is ΔE. $C_{m_p,n_r}(Q)$ is the tunneling matrix element from the nth level in the reactant state to the mth level in the product state. An explicit evaluation of the tunneling matrix element $C_{m_p,n_r}(Q)$ is obtained within the WKB semiclassical framework and is given by[15]

$$C_{m_p,n_r}(Q) = (h/4\pi^2)(\omega_R\omega_P)^{1/2}\exp\{(-2\pi^2/h\omega^\ddagger)[V^\ddagger - {}^1/_2(V_{n_r} + V_{m_p})]\} \tag{4}$$

where $\omega^\ddagger$ is a mass-weighted frequency associated with the inverted parabola of the transition state for the proton-transfer coordinate, $V^\ddagger$ is the energy of the transition state, and V_{n_r} and V_{m_p} are the energies of the reactant and the product states, which depend on the level of vibrational excitation in the two states.

Solvent Dependence of Nonadiabatic Proton Transfer. Recently, we reported a study of the correlation of the rates of proton transfer with driving force for a variety of substituted benzophenone/*N*,*N*-dimethylaniline contact triplet radical ion pairs in a series of nitrile solvents.[24] The correlation was examined within the context of Lee−Hynes theory, and it was found that the theory gave a good account of the kinetic behavior. The model incorporated as active vibrations the ground-state C−H stretch vibration, $n(0)$, in the reactant state and the O−H stretch vibration and its first overtone, $m(0)$ and $m(1)$, in the product state. During the fitting procedure it was assumed that there was no change in the internuclear separation between the reacting species upon proton transfer, leading to $\Delta Q = 0$.

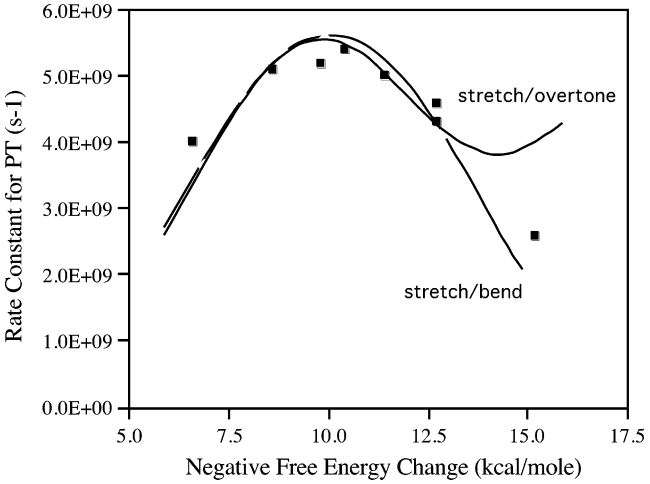

Figure 5. Plot of the experimental rate constants for proton transfer vs negative free energy change ($-\Delta G$, kcal/mol) for the solvent ethyl acetate. Key: squares, experimental data. Solid curve labeled stretch/overtone comes from the Lee−Hynes model with $E_\alpha = 1.0$ kcal/mol, $V^\ddagger = 17.5$ kcal/mol, $\omega_Q = 200$ cm^{-1}, $E_s = 9.1$ kcal/mol, $\Delta Q = 0.0$, $E_Q = 0.0$ kcal/mol, $\omega_R = 2701$ cm^{-1}, ω_P for $m(0) = 2386$ cm^{-1} (stretch), ω_P for $m(1) = 2 \times 2386$ cm^{-1} (overtone), and $\omega^\ddagger = 2500$ cm^{-1}. Solid curve labeled stretch/bend comes from the Lee−Hynes model with $E_\alpha = 1.0$ kcal/mol, $V^\ddagger = 19.5$ kcal/mol, $\omega_Q = 200$ cm^{-1}, $E_s = 9.1$ kcal/mol, $\Delta Q = 0.0$, $E_Q = 0.0$ kcal/mol, $\omega_R = 2701$ cm^{-1}, ω_P for $m(0) = 768$ cm^{-1} (bend), ω_P for $m(1) = 2386$ cm^{-1} (stretch), and $\omega^\ddagger = 2500$ cm^{-1}.

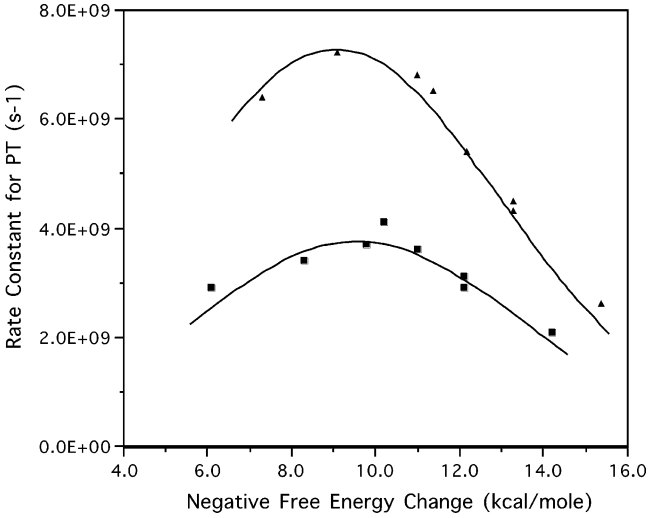

Figure 6. Plot of the experimental rate constants for proton transfer vs negative free energy change ($-\Delta G$, kcal/mol) for the solvent tetrahydrofuran and 1,2-dichloroethane. Key: triangles, experimental data for tetrahydrofuran; squares, experimental data for 1,2-dichloroethane. Solid curve for tetrahydrofuran comes from the Lee−Hynes model with $E_\alpha = 1.0$ kcal/mol, $V^\ddagger = 19.3$ kcal/mol, $\omega_Q = 200$ cm^{-1}, $E_s = 8.1$ kcal/mol, $\Delta Q = 0.0$, $E_Q = 0.0$ kcal/mol, $\omega_R = 2701$ cm^{-1}, ω_P for $m(0) = 768$ cm^{-1} (bend), ω_P for $m(1) = 2386$ cm^{-1} (stretch), and $\omega^\ddagger = 2500$ cm^{-1}. Solid curve for 1,2-dichlorethane comes from the Lee−Hynes model with $E_\alpha = 1.0$ kcal/mol, $V^\ddagger = 19.8$ kcal/mol, $\omega_Q = 202$ cm^{-1}, $E_s = 8.6$, $\Delta Q = 0.0$, $E_Q = 0.0$ kcal/mol, $\omega_R = 2701$ cm^{-1}, ω_P for $m(0) = 768$ cm^{-1} (bend), ω_P for $m(1) = 2386$ cm^{-1} (stretch), and $\omega^\ddagger = 2500$ cm^{-1}.

Employing the same fitting procedure, we applied the Lee−Hynes model to the kinetic data for the nonpolar solvents ethyl acetate, tetrahydrofuran, and 1,2-dichloroethane where the active vibrations in the product state are the O−H stretch vibration and its first overtone (stretch/overtone). The quality for the fit of the model to the kinetic data for this series of nonpolar solvents is inferior to that for nitrile solvents, as illustrated in Figure 5 for ethyl acetate. The difference between nonpolar and polar solvent data is that the nonpolar solvent data display a more pronounced inverted region. At large driving force (−15.2 kcal/mol), the rate constant for proton transfer within the 4,4′-dimethoxybenzophenone/DMA triplet contact radical ion pair is substantially slower than that predicted by the stretch/overtone model. The upturn in model calculation at large driving force is due to tunneling from the ground-state C−H stretch vibration into the first overtone of the O−H stretch vibration, $n(0) \rightarrow m(1)$. The experimental kinetic data for the more nonpolar solvents suggest that this vibration is not active in the proton tunneling process.

Assuming that only the zero-point vibrations of the O−H stretch and bend of the B configuration are active in the proton tunneling, we apply the Lee−Hynes model to the correlation of kinetic data with driving force for the solvent ethyl acetate. In modeling the tunneling matrix elements for transfer into the stretch and bend modes, lacking further information we assume that the barrier height, $V^\ddagger$, which serves as a fitting parameter is the same for the two modes. The barrier frequency is set to $\omega^\ddagger = 2500$, a value derived from a previous study of hydrogen atom transfer.[15] The energy term E_α is set to 1.0 kcal/mol; the procedure for estimating this value can be found in ref 1. Also, the vibrational frequency of the C−H transferring mode is set to 2701 cm^{-1}, a value derived from pBP/DN** calculations for DMA radical cation. For the low-frequency promoting mode, we assume a value of 200 cm^{-1} as no experimental data exist for intermolecular vibrations for contact radical ion pairs of this nature. With these assumptions and the assumption that $\Delta Q = 0$ leading to $E_Q = 0$, we find that the two-mode stretch and bend model (stretch/bend) gives a superior fit to the experimental data when compared to the two-mode model incorporating the O−H stretch and its overtone (Figure 5). The application of two-mode stretch and bend model to the remaining solvents is shown in Figures 6−8. The fitting procedure varies the solvent reorganization energy, E_s, the barrier height $V^\ddagger$, and the frequency of the promoting mode, ω_Q. The derived values for the fitting parameters are given in the respective figure captions.

It should be noted at this point that the present set of kinetic data is inadequate for assessing the contributions of vibrational overtones in the product state to the overall kinetics of proton transfer given the limited range in driving force. To address this issue, it will be necessary to employ experimental systems which can probe proton transfer in regime where the driving force is substantially greater than the present system can provide. An additional 9 kcal/mol of driving force would provide insight into the importance of overtone modes in proton transfer. Such molecular systems are currently under design.

Given the numerous assumptions employed in the Lee−Hynes analysis of the experimental kinetic data for the range of solvents, the quality of the correlation between the theoretical model and experiment is surprisingly good. However, one must approach the derived molecular parameters with caution. For example, there is a strong correlation between the barrier height $V^\ddagger$, the mass-weighted frequency of the transition state $\omega^\ddagger$, and low-frequency promoting mode ω_Q. For example, in pentanenitrile, if $\omega^\ddagger$ is increased from 2500 to 2800 cm^{-1}, the value of $V^\ddagger$ increases from 19.8 to 22.5 kcal/mol while a decrease in the promoting mode frequency ω_Q from 200 to 150 cm^{-1} leads to an increase in $V^\ddagger$ from 19.8 to 26.0 kcal/mol. Also, the position of the maximum rate constant for proton transfer in the correlation of rate constants with driving force is governed by the linear combination of E_α and E_s; thus, the derived values for E_s depends on the assumed value of E_α. With these caveats, it is apparent, given the quality of the correlation of the

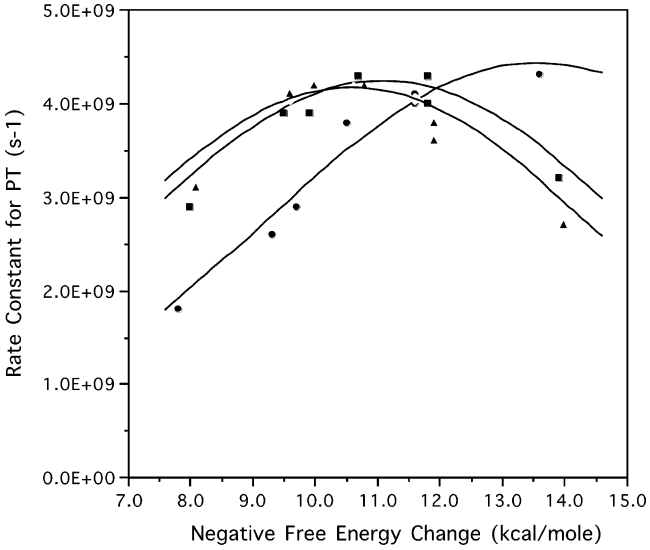

Figure 7. Plot of the experimental rate constants for proton transfer vs negative free energy change ($-\Delta G$, kcal/mol) for pentanenitrile, butanenitrile, and propanenitrile. Key: triangles, experimental data for pentanenitrile; squares, experimental data for butanenitrile; circles, experimental data for propanenitrile. Solid curve for pentanenitrile comes from the Lee−Hynes model with $E_\alpha = 1.0$ kcal/mol, $V^\ddagger = 19.8$ kcal/mol, $\omega_Q = 200$ cm^{-1}, $E_s = 9.6$ kcal/mol, $\Delta Q = 0.0$, $E_Q = 0.0$ kcal/mol, $\omega_R = 2701$ cm^{-1}, ω_P for $m(0) = 768$ cm^{-1} (bend), ω_P for $m(1) = 2386$ cm^{-1} (stretch), and $\omega^\ddagger = 2500$ cm^{-1}. Solid curve for butanenitrile comes from the Lee−Hynes model with $E_\alpha = 1.0$ kcal/mol, $V^\ddagger = 19.8$ kcal/mol, $\omega_Q = 199.5$ cm^{-1}, $E_s = 10.1$ kcal/mol, $\Delta Q = 0.0$, $E_Q = 0.0$ kcal/mol, $\omega_R = 2701$ cm^{-1}, ω_P for $m(0) = 768$ cm^{-1} (bend), ω_P for $m(1) = 2386$ cm^{-1} (stretch), and $\omega^\ddagger = 2500$ cm^{-1}. Solid curve for propanenitrile comes from the Lee−Hynes model with $E_\alpha = 1.0$ kcal/mol, $V^\ddagger = 19.8$ kcal/mol, $\omega_Q = 197.7$ cm^{-1}, $E_s = 12.6$ kcal/mol, $\Delta Q = 0.0$, $E_Q = 0.0$ kcal/mol, $\omega_R = 2701$ cm^{-1}, ω_P for $m(0) = 768$ cm^{-1} (bend), ω_P for $m(1) = 2386$ cm^{-1} (stretch), and $\omega^\ddagger = 2500$ cm^{-1}.

experimental data with the Lee−Hynes model, that the mechanism for proton transfer is a nonadiabatic process, and the solvent plays a determining role in controlling the dynamics of the transfer as evidenced by how the maximum rate depends on E_s. Transition-state theory and its semiclassical modification incorporating tunneling in the region of the transition state cannot account for the solvent dependence of these kinetic data.[9]

Solvent Dependence of the Inverted Region. For the Lee−Hynes model, as formulated in eq 3, the principal factor that controls the shape of the functional form for the correlation of the rate constant, $\ln k(n_r \rightarrow m_p)$, with driving force, ΔE, is the exponential term which contains the quadratic function A_1^2. Contained within this quadratic function are the driving force, ΔE, and the solvent reorganization energy, E_s, both of which will be sensitive to solvent polarity. The correlation of $\ln k(n_r \rightarrow m_p)$ as a function of ΔE should result in both a normal and an inverted region for proton transfer. This analytical form is reminiscent of the kinetic behavior of nonadiabatic electron transfer. The question that is pertinent to the present kinetic study of the correlation of the rate of proton transfer with driving force is how does the functional form change with solvent polarity; i.e., should the peak in the correlation function vary with solvent polarity?

Wasielewski and co-workers[34] have modeled the functional dependence of the normal and inverted regions with a change in solvent polarity for nonadiabatic electron transfer for a system that involves the decay of charge-separated species in donor−acceptor molecules to form neutral species. The driving force, ΔE, and solvent reorganization energy, E_s, were modeled within

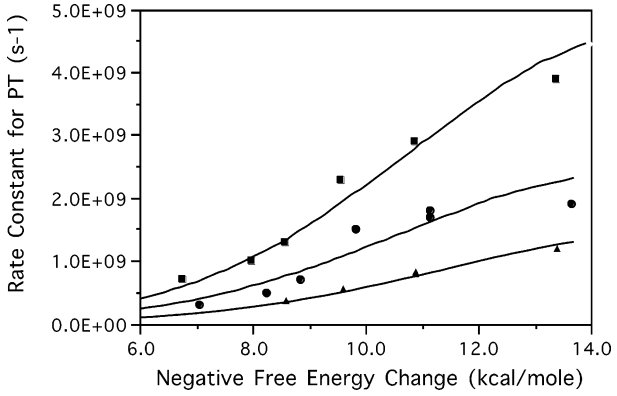

Figure 8. Plot of the experimental rate constants for proton transfer vs negative free energy change ($-\Delta G$, kcal/mol) for acetonitrile, dimethylformamide, and dimethyl sulfoxide. Key: squares, experimental data for acetonitrile; circles, experimental data for dimethylformamide; triangles, experimental data for dimethyl sulfoxide. Solid curve for acetonitrile comes from the Lee−Hynes model with $E_\alpha = 1.0$ kcal/mol, $V^\ddagger = 19.8$ kcal/mol, $\omega_Q = 194$ cm^{-1}, $E_s = 16.6$ kcal/mol, $\Delta Q = 0.0$, $E_Q = 0.0$ kcal/mol, $\omega_R = 2701$ cm^{-1}, ω_P for $m(0) = 768$ cm^{-1} (bend), ω_P for $m(1) = 2386$ cm^{-1} (stretch), and $\omega^\ddagger = 2500$ cm^{-1}. Solid curve for dimethylformamide comes from the Lee−Hynes model with $E_\alpha = 1.0$ kcal/mol, $V^\ddagger = 20.5$ kcal/mol, $\omega_Q = 200.0$ cm^{-1}, $E_s = 14.6$ kcal/mol, $\Delta Q = 0.0$, $E_Q = 0.0$ kcal/mol, $\omega_R = 2701$ cm^{-1}, ω_P for $m(0) = 768$ cm^{-1} (bend), ω_P for $m(1) = 2386$ cm^{-1} (stretch), and $\omega^\ddagger = 2500$ cm^{-1}. Solid curve for dimethyl sulfoxide comes from the Lee−Hynes model with $E_\alpha = 1.0$ kcal/mol, $V^\ddagger = 20.9$ kcal/mol, $\omega_Q = 200$ cm^{-1}, $E_s = 15.6$ kcal/mol, $\Delta Q = 0.0$, $E_Q = 0.0$ kcal/mol, $\omega_R = 2701$ cm^{-1}, ω_P for $m(0) = 768$ cm^{-1} (bend), ω_P for $m(1) = 2386$ cm^{-1} (stretch), and $\omega^\ddagger = 2500$ cm^{-1}.

a dielectric continuum framework. They found that as the solvent dielectric constant increases, the driving force ΔE decreases at the same rate that the solvent reorganization energy E_s increases. Thus, the prediction within a dielectric continuum model for nonadiabatic electron transfer is that as the solvent polarity increases, the peak in the correlation function remains unchanged; only the width of the correlation is sensitive to the solvent polarity.

In a series of experimental studies on electron transfer in donor−acceptor systems, Gould, Farid, and co-workers have ascertained how the driving force for charge recombination in the 1,2,4,5-tetracyanobenzene−hexamethylbenzene contact radical ion pair changes with solvent polarity.[31,35] In addition, from the analysis of emission profile of the 1,2,4,5-tetracyanobenzene/hexamethylbenzene contact radical ion pair, the polarity dependence of the solvent reorganization energy was ascertained. As an example, when the solvent was changed from carbon tetrachloride to chloroform, an increase in polarity, the driving force for charge recombination decreased by 4.1 kcal/mol while the solvent reorganization energy increased by 8.5 kcal/mol. This behavior does not follow the predictions of the dielectric continuum model as the changes in the two terms do not offset one another.

Given that solvent reorganization energy increases to a greater extent than the driving force decreases in charge recombination reactions with an increase in solvent polarity, it is anticipated similar behavior should be found for proton-transfer reactions involving the decay of radical ion pairs to form radical pairs. As a consequence, if nonadiabatic proton transfer displays a normal and inverted region in the correlation of $\ln k(n_r \rightarrow m_p)$ as a function of ΔE, then as the solvent polarity increases, the peak in the correlation function should shift to larger negative free energies. This behavior is observed for the polarity dependence of the kinetics of proton transfer within the benzophenone/*N*,*N*-dimethylaniline contact triplet radical ion

pairs (Figures 5−8). For the solvents tetrahydrofuran, ethyl acetate, 1,2-dichloroethane, pentanenitrile, and butanenitrile, whose E_T30 values range from 37.4 to 43.1, the maximum rate of proton transfer progressively shifts to larger negative free energies as the solvent polarity increases. For the solvents propanenitrile, acetonitrile, dimethylformamide, and dimethyl sulfoxide, whose E_T30 values exceed 43.8, the maximum rate has shifted to such a large value of driving force that the inverted region is no longer observed experimentally given the limited range in driving forces that are accessible.

Kinetic Deuterium Isotope Effect. The Lee−Hynes model for nonadiabatic proton transfer is equally applicable to deuteron transfer. Three of the molecular parameters contained within the theory are sensitive to the mass of the transferring particle. The term E_α, eq 2, depends on the mass of transferring particle through its dependence on α, the exponential decay parameter for the tunneling matrix element. Since the tail of the deuteron wave function falls off more rapidly than that for the proton, α_D is greater than α_H by a factor of $\sqrt{2}$, leading to an increase by a factor of 2 in the E_α for deuteron transfer relative to proton transfer.[36] Since the maximum in the correlation of the rate constants with driving force is controlled by the linear combination of E_α and E_s, the exchange of a deuteron for a proton will produce a shift of the maximum rate constant for the transfer to a larger driving force. Experimental observation of such a shift would support the role of intermolecular vibrations in modulating the tunneling matrix elements. The remaining mass-dependent parameters are the mass-weighted barrier frequency, $\omega^\ddagger$, which will be reduced by a factor of $1/\sqrt{2}$ and a shift in vibrational frequencies and zero-point energies of the transferring modes.

Applying the Lee−Hynes model for deuteron transfer in the solvent pentanenitrile and butanenitrile, we increased the E_α value from 1 to 2 kcal/mol and reduced the C−H transferring mode from 2701 to 1910 cm^{-1}. The two receiving modes in the product state were reduced from 2386 to 1687 cm^{-1} and from 768 to 543 cm^{-1}. The mass-weighted barrier frequency, $\omega^\ddagger$, is reduced from 2500 to 1768 cm^{-1}. The only variable fitting parameter is the barrier height, $V^\ddagger$. In fitting the theoretical model to the proton-transfer data, we defined $V^\ddagger$ as the energy difference between the top of barrier and the zero-point energy of the C−H transferring vibrational mode. Upon deuteration, the zero-point energy should be reduced by a factor of $\sqrt{2}$, leading to an increase in $V^\ddagger$. Since for proton transfer the derived value for $V^\ddagger$ was 19.8 kcal/mol in pentanenitrile and butanenitrile, it is anticipated that the value for $V^\ddagger$ should be 20.9 kcal/mol for deuteron transfer in these two solvents.

The fit of the Lee−Hynes model to the kinetic data for deuteron transfer for pentanenitrile and butanenitrile is shown in Figures 9 and 10. For comparison, the kinetic data and the associated fit of the model for proton transfer are included. With $V^\ddagger$ as the only adjustable parameter, the derived value for $V^\ddagger$ is 20.1 kcal/mol for both sets of kinetic data, a value that is very close to the anticipated value of 20.9 kcal/mol. Also, examining the maximum in the rate data for proton and deuteron transfer, the position of maximum is clearly shifted to higher energies for deuteron transfer, reflecting the increase in E_α upon deuteration as predicted by theory. Overall, the Lee−Hynes model for proton/deuteron nonadiabatic transfer gives a remarkable account of the observed kinetic behavior for proton/deuteron transfer in the benzophenone/*N*,*N*-dimethylaniline triplet contact radical ion pair as a function of solvent.

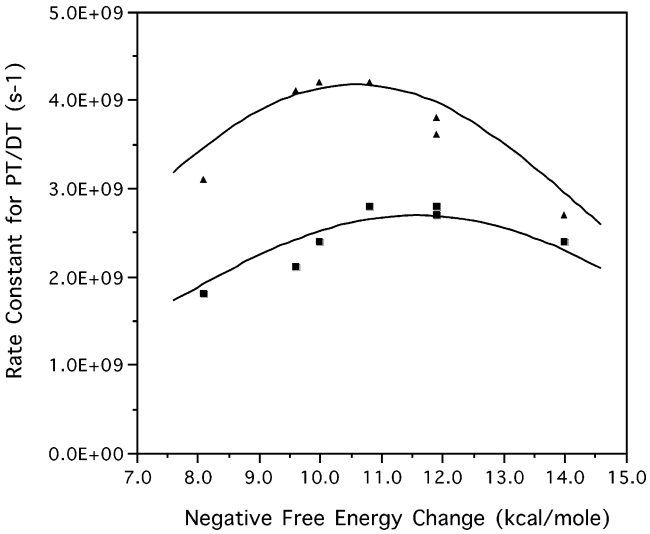

Figure 9. Plot of the experimental rate constants for proton transfer from *N*,*N*-dimethylaniline cation radical and deuteron transfer from *N*,*N*-dimethyl-d_6-aniline cation radical vs negative enthalpy change (−Δ*E*, kcal/mol) in pentanenitrile. Key: triangles, experimental data for proton transfer; squares, experimental data for deuteron transfer. Solid curve deuteron transfer comes from the Lee−Hynes model with $E_\alpha = 2.0$, $V^\ddagger = 20.1$ kcal/mol, $\omega_Q = 200$ cm^{-1}, $E_s = 9.6$, $\Delta Q = 0.0$, $E_Q = 0.0$, $\omega_R = 1901$ cm^{-1}, ω_P for $m(0) = 543$ cm^{-1} (bend), ω_P for $m(1) = 1687$ cm^{-1} (stretch), and $\omega^\ddagger = 1768$ cm^{-1}. Solid curve for proton transfer in pentanenitrile comes from parameters given in Figure 7.

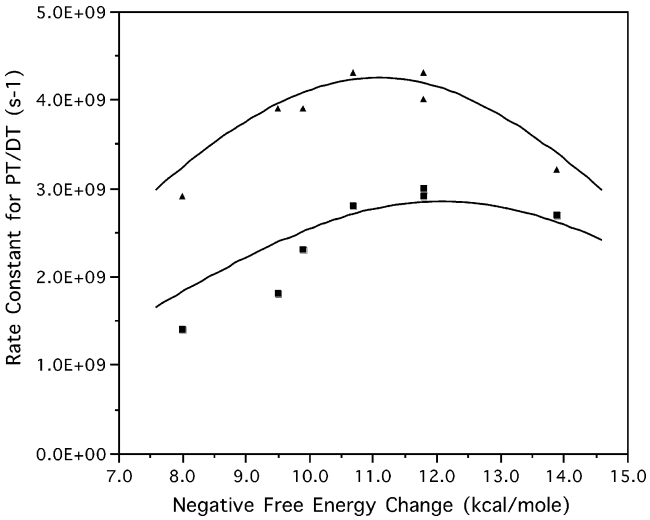

Figure 10. Plot of the experimental rate constants for proton transfer from *N*,*N*-dimethyaniline cation radical and deuteron transfer from *N*,*N*-dimethyl-d_6-aniline cation radical vs negative enthalpy change (−Δ*E*, kcal/mol) in butanenitrile. Key: squares, experimental data for proton transfer; circles, experimental data for deuteron transfer. Solid curve deuteron transfer comes from the Lee−Hynes model with $E_\alpha = 2.0$, $V^\ddagger = 20.1$ kcal/mol, $\omega_Q = 199$ cm^{-1}, $E_s = 10.1$, $\Delta Q = 0.0$, $E_Q = 0.0$, $\omega_R = 1901$ cm^{-1}, ω_P for $m(0) = 543$ cm^{-1} (bend), ω_P for $m(1) = 1687$ cm^{-1} (stretch), and $\omega^\ddagger = 1768$ cm^{-1}. Solid curve for proton transfer in butanenitrile comes from parameters given in Figure 7.

Conclusions

The rationalization of the solvent dependence for the kinetics of proton/deuteron transfer within the benzophenone/*N*,*N*-dimethylaniline triplet contact radical ion pairs presents a unique challenge for theoretical models of proton-transfer processes. The nonadiabatic theory of Lee and Hynes gives a good account for the both the solvent dependence and the kinetic deuterium isotope effect. The observed shift to a larger driving force for the maximum rate constant of transfer that occurs upon replacing

the proton by a deuteron can be rationalized with the Lee−Hynes model as due to a change in E_α upon deuteration. This shift supports the theoretical assertion that low-frequency intermolecular vibrational modes modulate the tunneling dynamics, reflecting the extreme sensitivity of the distance dependence of tunneling matrix element. Also, the low values of the kinetic deuterium isotope effect, values ranging from 1.1 to 2.0, are in accord with Lee−Hynes theory. Thus, low values for the kinetic deuterium isotope effect cannot be used to rule out tunneling processes in proton transfer reactions as has been traditionally asserted.

The proton transfer process within the benzophenone/*N*,*N*-dimethylaniline contact radical ion pair appears to be the first molecular system which clearly illustrates nonadiabatic proton transfer at ambient temperatures in the condense phase However, caution must be exercised in attempting to extrapolate the observed kinetic behavior for this system to proton transfer in other intermolecular systems although recently Saveant and coworkers observed an inverted region in proton transfer to the diphenylmethyl carbanion.[37] The unique π-stacked structure of the triplet contact radical ion pair serves to fix the internuclear separation of the two heavy atoms that bound the proton transfer. Removing the distance constraints would allow for the two heavy atoms to move closer together, reducing the distance of proton transfer. At short distances the electronic barrier to proton transfer may be reduced to a level below the zero-point energy of the vibration associated with the transferring proton so that the transfer process shifts from the nonadiabatic regime to the adiabatic regime. The solvent dependence and kinetic deuterium isotope effects differ in these two regimes.

Acknowledgment. This work is supported by grants from the National Science Foundation, CHE-9816540, and the Cristol Fund administered by the Department of Chemistry and Biochemistry at the University of Colorado.

References and Notes

(1) Borgis, D.; Hynes, J. T. *J. Phys. Chem.* **1996**, *100*, 1118.
(2) Kohen, A.; Klinman, J. P. *Acc. Chem. Res.* **1998**, *31*, 397.
(3) Kuznetsov, A. M. *Charge Transfer in Physics, Chemistry and Biology*; Gordon and Breach: Luxembourg, 1995.
(4) Cukier, R. I.; Morillo, M. *J. Chem. Phys.* **1989**, *91*, 857.
(5) Lobaugh, J.; Voth, G. A. *J. Chem. Phys.* **1994**, *100*, 3039.
(6) Hammes-Schiffer, S.; Tully, J. C. *J. Chem. Phys.* **1994**, *101*, 4657.
(7) Hammes-Schiffer, S. *Acc. Chem. Res.* **2001**, *34*, 273.
(8) Bell, R. P. *The Proton in Chemistry*; Chapman and Hall: London, 1973.
(9) Bell, R. P. *The Tunnel Effect in Chemistry*; Chapman and Hall: London, 1980.
(10) Borgis, D.; Hynes, J. T. *The Enzyme Catalysis Process*; Plenum: New York, 1989.
(11) Borgis, D. C.; Lee, S.; Hynes, J. T. *Chem. Phys. Lett.* **1989**, *162*, 19.
(12) Borgis, D.; Hynes, J. T. *J. Chem. Phys.* **1991**, *94*, 3619.
(13) Morillo, M.; Cukier, R. I. *J. Chem. Phys.* **1990**, *92*, 4833.
(14) Li, D.; Voth, G. A. *J. Phys. Chem.* **1991**, *95*, 10425.
(15) Lee, S.; Hynes, J. T. *J. Chim. Phys.* **1996**, *93*, 1783.
(16) Barbara, P. F.; Walsh, P. K.; Brus, L. E. *J. Phys. Chem.* **1989**, *93*, 29.
(17) Pines, E.; Fleming, G. R. *Chem. Phys.* **1994**, *183*, 393.
(18) Pines, E.; Magnes, B.; Lang, M. J.; Fleming, G. R. *Chem. Phys. Lett.* **1997**, *281*, 413.
(19) Zewail, A. H. *J. Phys. Chem.* **1996**, *100*, 12701.
(20) Hineman, M. F.; Bruker, G. A.; Kelley, D. F.; Bernstein, E. R. *J. Chem. Phys.* **1990**, *92*, 805.
(21) Brucker, G. A.; Swinney, T. C.; Kelley, D. F. *J. Phys. Chem.* **1991**, *95*, 3190.
(22) Peters, K. S.; Cashin, A.; Timbers, P. *J. Am. Chem. Soc.* **2000**, *122*, 107.
(23) Peters, K. S.; Cashin, A. *J. Phys. Chem. A* **2000**, *104*, 4833.
(24) Peters, K. S.; Kim, G. *J. Phys. Chem. A* **2001**, *105*, 4177.
(25) Manring, L. E.; Peters, K. S. *J. Am. Chem. Soc.* **1985**, *107*, 6452.
(26) Peters, K. S.; Lee, J. *J. Phys. Chem.* **1992**, *96*, 8941.
(27) Hehre, W. J.; Yu, J.; Klunzinger, P. E.; Lou, L. *A Brief Guide to Molecular Mechanics and Quantum Chemical Calculations*; Wavefunction, Inc: Irvine, CA, 1998.
(28) Peters, K. S. Proton-Transfer Reactions in Benzophenone/N,N-Dimethylaniline Photochemistry. In *Advances in Photochemistry*; Neckers, D. C., Ed.; John Wiley & Sons: New York, 2002; Vol. 27, p 51.
(29) Parker, V. D.; Tilset, M. *J. Am. Chem. Soc.* **1991**, *113*, 8778.
(30) Arnaut, L. G.; Caldwell, R. A. *J. Photochem. Photobiol. A: Chem.* **1992**, *65*, 15.
(31) Arnold, B. R.; Farid, S.; Goodman, J. L.; Gould, I. R. *J. Am. Chem. Soc.* **1996**, *118*, 5482.
(32) Leigh, W. J.; Arnold, D. R.; Humphreys, R. W. R.; Wong, P. C. *Can. J. Chem.* **1980**, *58*, 2537.
(33) Miyasaka, H.; Morita, K.; Kamada, K.; Mataga, N. *Bull. Chem. Soc. Jpn.* **1990**, *63*, 3385.
(34) Wasielewski, M. R.; Gaines, G. L.; O'Neil, M. P.; Svec, W. A.; Niemczyk, M. P.; Prodi, L.; Gosztola, D. Solvent Effects on the Rate vs Free Energy Dependence of Photoinduced Charge Separation in Fixed Donor−Acceptor Molecules. In *Dynamics and Mechanims of Photoinduced Transfer and Related Phenomena*; Mataga, N., Okada, T., Masuhara, H., Eds.; Elsevier Science Publishers: New York, 1992; p 87.
(35) Gould, I. R.; Noukakis, D.; Gomez-Jahn, L.; Young, R. H.; Goodman, J. L.; Farid, S. *Chem. Phys.* **1993**, *176*, 439.
(36) Hynes, J. T. Personal communication.
(37) Andrieux, C. P.; Gamby, J.; Hapiot, P.; Saveant, J. M. *J. Am. Chem. Soc.* **2003**, *125*, 10119.